# Wireless gas detection with a smartphone via rf communication

Joseph M. Azzarelli, Katherine A. Mirica, Jens B. Ravnsbæk[1], and Timothy M. Swager[2]

Department of Chemistry, Massachusetts Institute of Technology, Cambridge, MA 02139

Edited by Chad A. Mirkin, Northwestern University, Evanston, IL, and approved November 5, 2014 (received for review August 10, 2014)

**Chemical sensing is of critical importance to human health, safety, and security, yet it is not broadly implemented because existing sensors often require trained personnel, expensive and bulky equipment, and have large power requirements. This study reports the development of a smartphone-based sensing strategy that employs chemiresponsive nanomaterials integrated into the circuitry of commercial near-field communication tags to achieve non-line-of-sight, portable, and inexpensive detection and discrimination of gas-phase chemicals (e.g., ammonia, hydrogen peroxide, cyclohexanone, and water) at part-per-thousand and part-per-million concentrations.**

RFID | NFC | sensor | nanomaterials | wireless

Portable chemical sensors are needed to manage and protect the environment (1), human health (2, 3), and quality of life (4). Examples include sensors for point-of-care diagnosis of disease (5), detection of explosives and chemical warfare agents (6), indication of food ripening and spoilage (7), and monitoring of environmental pollution (1). Connecting sensors with information technology through wireless rf communication is a promising approach to enable cost-effective onsite chemical detection and analysis (8). Although rf technology has been recently applied toward wireless chemical sensing, current approaches have several limitations, including lack of specificity to selected chemical analytes, requirements for expensive, bulky, fragile, and operationally complex impedance and network analyzers, and reliance on extensive data processing and analysis (8–13). We report herein the adaptation of a nascent technology embedded in modern smartphones—near-field communication (NFC)—for wireless electronic, portable, non-line-of-sight selective detection of gas-phase chemicals (Fig. 1 and Fig. S1). We demonstrate this concept by (*i*) incorporating carbon-based chemiresponsive materials into the electronic circuitry of commercial NFC tags by mechanical drawing and (*ii*) using an NFC-enabled smartphone to relay information regarding the chemical environment (e.g., presence or absence of a chemical) surrounding the NFC tag. This paper illustrates the ability to detect and differentiate part-per-million (ppm) concentrations of ammonia, cyclohexanone, and hydrogen peroxide. We demonstrate the ability to couple wireless acquisition and transduction of chemical information with existing smartphone functions [e.g., Global Positioning System (GPS)] (Movie S1).

Many commercial smartphones and mobile devices are equipped with NFC hardware configured to communicate wirelessly with NFC "tags"—simple electrical resonant circuits comprising inductive ($L$), capacitive ($C$), and resistive ($R$) elements on a plastic substrate (Fig. 1). The smartphone, such as the Samsung Galaxy S4 (SGS4) used in this study, communicates with the battery-free tag by powering its integrated circuit (IC) via inductive coupling at 13.56 MHz (14). Power transferred from the smartphone to the IC is, among other variables, a function of the transmission frequency ($f$), the resonant frequency ($f_0$), the quality factor ($Q$), and the circuit efficiency ($\eta$), which in turn are functions of $L$ (H), $C$ (F), and $R$ (Ω) of the smartphone and NFC resonant circuit components (15). Integration of chemiresponsive materials into commercial NFC tags produces stimuli-responsive variable circuit components that affect power transfer between the tag and a smartphone in the presence or absence of chemical stimuli. The resulting programmable chemically actuated resonant devices (CARDs) enable non-line-of-sight smartphone chemical sensing by disrupting or allowing rf communication.

## Fabrication and Characterization of CARDs

We render commercial NFC tags chemically sensitive via a simple two-step modification procedure (Fig. 1). First, we disrupt the electronic circuit of the tag, rendering the tag unreadable, by removing a section of the conductive aluminum that connects the IC to the capacitor with a hole puncher. Then, we recomplete the $LCR$ circuit with conductive nanocarbon-based chemiresponsive materials deposited by mechanical abrasion (16) (Fig. 1). We achieve chemical selectivity in sensing by harnessing the established properties of chemiresponsive materials (16–18).

This study used two different solid-state chemiresponsive materials—PENCILs (process-enhanced nanocarbon for integrated logic)—that can be conveniently drawn on a variety of surfaces using an established technique (17). For sensing ammonia ($NH_3$) and hydrogen peroxide ($H_2O_2$)—common industrial hazards that can be used in improvised explosives—we chose pristine single-walled carbon nanotubes (SWCNTs) compressed in the form of a pencil "lead" (16, 18) (**P1**); this material exhibits a well-characterized, dose-dependent chemiresistive response toward these analytes. We also chose a solid composite comprising a 4:1 (wt:wt) blend of 2-(2-hydroxy-1,1,1,3,3,3-hexafluoropropyl)-1-naphthol (HFIPN) with SWCNTs generated via solvent-free mechanical mixing within a ball mill (**P2**) because this material exhibits high selectivity and sensitivity for

## Significance

**This paper describes the first example of an adaption of near-field communication (NFC) technology—in 0.5 billion modern smartphones and mobile devices installed in 2014—toward portable, wireless, non-line-of-sight gas phase chemical sensing. We demonstrate the ability to convert inexpensive commercial NFC tags into chemical sensors that detect and discriminate analytes at part-per-thousand and part-per-million concentrations. This effort merges rational design of conductive nanostructured materials for selective chemical sensing with portable and widely distributed NFC technology to deliver a new method of acquiring chemical information about an NFC tag's local environment. This paper introduces a concept for distributed chemical sensing by the growing number of people that carry NFC-enabled smartphones, tablets, and other smart devices.**

Author contributions: J.M.A., K.A.M., J.B.R., and T.M.S. designed research; J.M.A., K.A.M., and J.B.R. performed research; J.M.A., K.A.M., J.B.R., and T.M.S. analyzed data; and J.M.A., K.A.M., J.B.R., and T.M.S. wrote the paper.

Conflict of interest statement: A patent has been filed on this technology.

This article is a PNAS Direct Submission.

[1]Present address: Chemistry and Biotechnology, Life Science, Danish Technological Institute, DK-8000 Aarhus, Denmark.

[2]To whom correspondence should be addressed. Email: tswager@mit.edu.

This article contains supporting information online at www.pnas.org/lookup/suppl/doi:10.1073/pnas.1415403111/-/DCSupplemental.

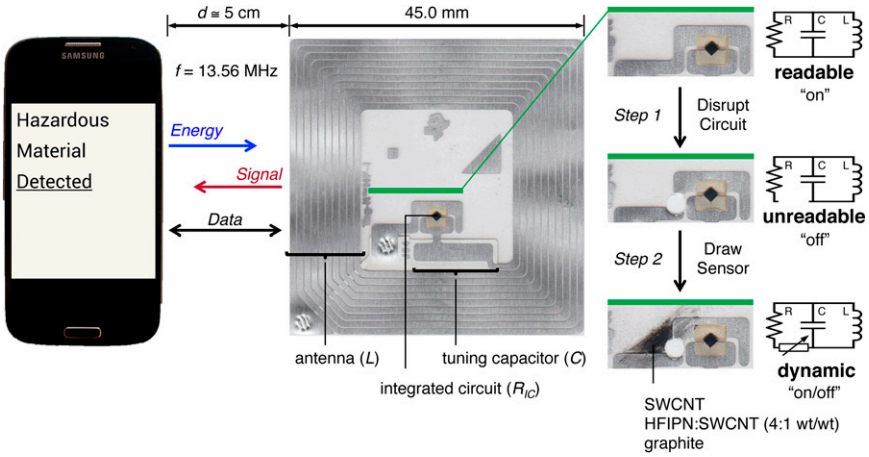


**Fig. 1.** Conversion of an NFC tag into a CARD enables wireless rf detection of chemical analytes with a smartphone. NFC-enabled smartphones communicate with NFC tags by simultaneously energizing the NFC tag with an alternating magnetic field ($f$ = 13.56 MHz) through inductive coupling and transferring data by signal modulation. NFC tags are converted into **CARD**s by disrupting the *LCR* circuit (step 1) and recompleting the circuit with a stimuli-responsive variable circuit component by drawing (step 2) with solid sensing materials.

cyclohexanone ($C_6H_{10}O$) vapors (a common constituent of plastic explosives) (17, 19, 20). HB pencil lead (**P3**) was chosen as a negative control because it shows a negligible response toward the concentrations of analytes used in this study. These materials exhibit predictable drift and consistent stability in their electrical resistance ($R_s$) when deposited on the surface of the NFC tags (Figs. S2 and S3).

We used a network analyzer to determine $f_0$ and $Q$ of the NFC tags at various stages of modification by measuring the rf reflection coefficient, $S_{11}$ (Fig. 2 and Fig. S4) (21). In tandem, we also used SGS4 to test the readability of the tags ("on"/"readable" and "off"/"unreadable") and a multimeter to estimate the electrical resistance ($R_s$) of the connection between the capacitor and the integrated circuit within the NFC tag (Fig. S5). Fig. 2*A* shows a plot that exhibits six notable features. First, in the absence of any device, the $S_{11}$ spectrum displays a flat baseline (Fig. 2 *A*, *1*). Second, unmodified NFC tags ($R_s$ = 0.3 Ω ± 0.0 Ω) are SGS4-readable (on) and display a resonant frequency of 13.67 ± 0.01 MHz and $Q$ = 35 ± 1 (Fig. 2 *A*, *2*). Third, tags where the electrical connection between the integrated circuit and the capacitor has been disrupted by hole punching ($R_s$ = 23.3 ± 0.8 MΩ) are SGS4-unreadable (off) and display $f_0$ = 14.29 ± 0.01 MHz and $Q$ = 85 ± 2 (Fig. 2 *A*, *3*). Fourth, when the electrical circuit is recompleted using **P2**, the resulting **CARD-2** ($R_s$ = 16.5 ± 1.0 kΩ) becomes SGS4-readable (on) and has $f_0$ = 14.26 ± 0.02 MHz and $Q$ = 21 ± 1 (Fig. 2 *A*, *4*). Fifth, when this **CARD-2** is exposed to vapors of cyclohexanone (~5,000 ppm), a significant change in both $f_0$ and $Q$ is observed. After 5 s of exposure, $f_0$ shifts to 14.30 ± 0.01 MHz and $Q$ increases to 32 ± 1 (Fig. 2 *A*, *5*), and the tag becomes SGS4-unreadable (off). After 1 min, $f_0$ remains at 14.30 ± 0.00 MHz; $Q$ increases to 51 ± 2 (Fig. 2 *A*, *6*), and the tag remains SGS4-unreadable (off).

Readability of CARDs by the smartphone can be rationalized by estimating the percent of incident power transferred ($P_t$) from the smartphone to the tag or CARD (Fig. 2*B* and Fig. S6). For the purposes of this study, the distance of the smartphone to the CARD and the orientation of the smartphone with respect to the CARD were kept constant (*Methods*); however, in a non-laboratory setting distance and orientation would have to be taken into consideration. The commercial NFC tag (Fig. 2 *B*, *2*) absorbs nearly 77% of the rf signal delivered from the smartphone. The disrupted circuit, however, absorbs only 14% of the rf signal from the phone; this amount is insufficient for effective smartphone–tag communication and the tag is unreadable by the SGS4 (Fig. 2 *B*, *3*). Incorporation of a chemiresponsive material from **P2** into this tag creates **CARD-2**, resulting in the amount of absorbed rf signal increasing to 23%—a sufficient amount of power transfer to enable rf communication (on) (Fig. 2 *B*, *4*). Subsequent exposure of **CARD-2** to $C_6H_{10}O$ decreases the absorbed rf signal to 19% and results in **CARD-2** becoming unreadable by SGS4 (Fig. 2 *B*, *5*). Prolonged exposure of **CARD-2** to the

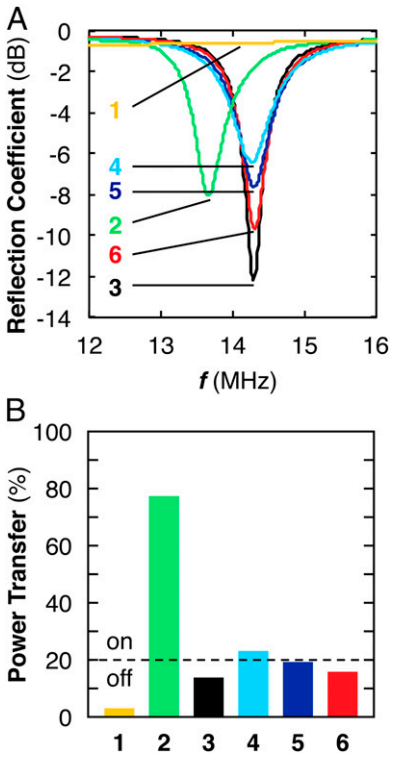


**Fig. 2.** The presence of an analyte influences the power transfer between the smartphone and CARD. (*A*) Average ($n$ = 5) reflection coefficient ($S_{11}$) of (1) baseline (no tag present), (2) unmodified NFC tag, (3) circuit-disrupted tag, (4) **CARD-2**, or (5) **CARD-2** in the presence of cyclohexanone (equilibrium vapor pressure at ambient temperature and pressure) for 5 s and (6) for 1 min. (*B*) Average ($n$ = 5) estimated power transfer ($P_t$) (13.53–13.58 MHz) from SGS4 to CARDs described in 1–6.

ENGINEERING

analyte for 1 min leads to a further decrease in absorbed rf signal from the phone (16%) (Fig. 2 *B*, *6*). Thus, $P_t$ between smartphone and CARDs decreases with increasing $R_s$.

### Semiquantitative Detection of Ammonia with a Smartphone and CARDs

After establishing the correlation between $R_s$, $P_t$, and the readability by the smartphone, we tested the ability of CARDs to detect and wirelessly communicate repeated chemical exposure to 35 ppm $NH_3$ gas. To program CARDs ($n = 3$) for $NH_3$, we integrated **P1** with initial $R_s = 16.1 \pm 0.6$ kΩ into the *LCR* circuit using the modification method described in Fig. 1, resulting in **CARD-1A**. We measure $R_s$ and test the SGS4 readability of **CARD-1A** in response to four consecutive exposures to 35 ppm $NH_3$ gas (Fig. S7). For clarity, Fig. 3*A* summarizes the effect of $NH_3$ (35 ppm) on the resistance and phone readability of a single **CARD-1A**. Within 1 min of exposure to 35 ppm $NH_3$, **CARD-1A** experienced $\Delta R_s = 5.3 \pm 0.7$ kΩ and became unreadable (turned off) when probed by the phone. Removal of $NH_3$ and recovery under ambient air led to a rapid recovery of $R_s$ and retrieval of phone readability of **CARD-1A**. After a 20-min recovery under ambient atmosphere, the $R_s$ of **CARD-1A** recovered to $17.4 \pm 0.6$ kΩ ($\Delta R_s = +1.2 \pm 0.3$ kΩ from the value of $R_s$ before exposure).

Correlating the readability of **CARD-1A** by SGS4 with $R_s$ enabled us to estimate that the on/off threshold ($R_t$) for **P1** when exposed to $NH_3$ was $20.8 \pm 1.0$ kΩ (*Supporting Information* and Table S1). Below this critical value of $R_t$, **CARD-1A** was readable by the SGS4, and we have established that it is unreadable when $R_s > R_t$. The well-defined value of $R_t$ in the wireless communication between the smartphone and CARDs fabricated with **P1**, coupled with the established concentration-dependent response of SWCNTs to $NH_3$, enables semiquantitation. To demonstrate this concept, we fabricated, in triplicate, two types of CARDs designed to turn off in response to crossing different threshold concentrations of $NH_3$: 4 ppm (just below the threshold of human detection of $NH_3$ based on smell) (**CARD-1B**; initial $R_s = 19.2 \pm 0.2$ kΩ) and 35 ppm [National Institute of Occupational Safety and Health (NIOSH) short-term exposure limit (STEL)] (**CARD-1A**; initial $R_s = 16.3 \pm 0.5$ kΩ) (Fig. 3*B* and Fig. S8). Before exposure to $NH_3$, both CARDs were readable by the phone. Exposure to 4 ppm $NH_3$ only turns **CARD-1B** off, whereas exposure to 35 ppm $NH_3$ turns both CARDs off. This concept is general: With sufficient information about the concentration-dependent response of the chemiresponsive sensing elements in the presence of the analytes of interest, CARDs can be programmed to turn on or off at the designated thresholds of various analytes.

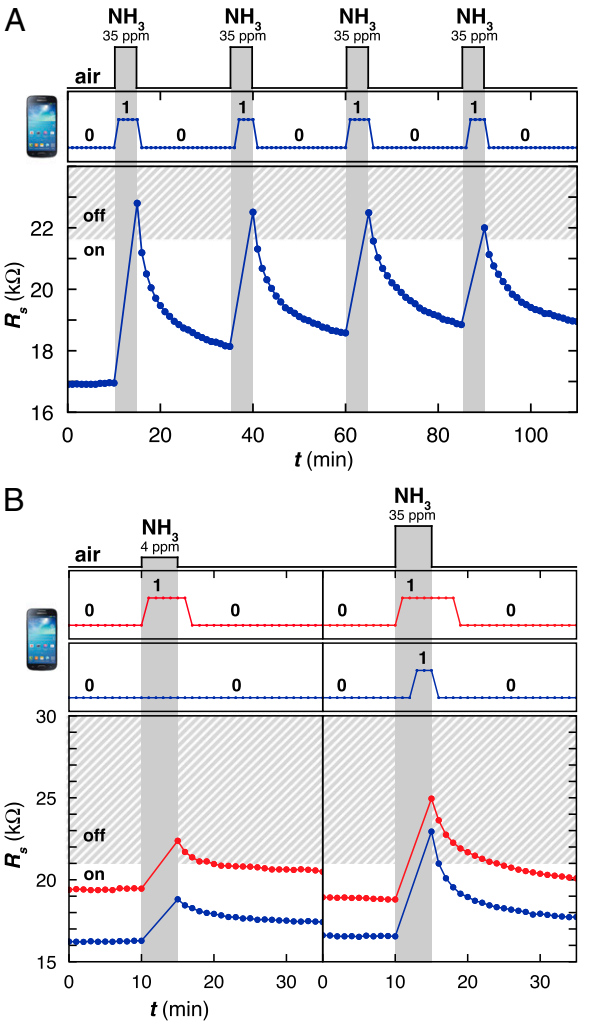


**Fig. 3.** CARDs can be programmed to detect different concentrations of analyte. (*A*) Response of **CARD-1A** to four 5-min exposures of $NH_3$ (35 ppm) at 20-min intervals as monitored with a SGS4 (*Top*) and a multimeter (*Bottom*). Shaded boundary indicates estimated $R_t$ based on the trace shown. (*B*) Response of **CARD-1A** (blue) and **CARD-1B** (orange) to a single 5-min exposure of $NH_3$ at two different concentrations (4 ppm and 35 ppm) as monitored with a SGS4 (*Top*) and a multimeter (*Bottom*). Shaded boundary indicates estimated $R_t$ based on the traces shown.

### Discrimination of Analytes with an Array of CARDs

The fabrication of arrays of CARDs containing different chemiresponsive materials can also enable the detection and discrimination of multiple analytes using NFC communication (Fig. 4). We used three different sensing materials (**P1**–**P3**) that produce distinct $\Delta R_s$ upon interaction with $NH_3$ gas (35 ppm), cyclohexanone vapor (335 ppm), $H_2O_2$ vapor (~225 ppm), and $H_2O$ vapor (~30,000 ppm). We produced an array of four types of CARDs (each type in triplicate) and used these devices to detect single exposures of the analytes. To detect $NH_3$, we used **CARD-1A** (initial $R_s = 16.3 \pm 0.6$ kΩ) designed to turn off upon exposure to 35 ppm $NH_3$ and turn back on upon recovery under ambient conditions (Fig. 4 *A*, *1*). Importantly, **CARD-1A** does not turn off in the presence of the other analytes at the concentrations tested (Fig. 4 *A*, *2*–*4*).

To detect $H_2O_2$, we fabricated a "turn-on" sensor having an initial condition of being off by mechanically abrading **P1** to obtain initial $R_s = 23.4 \pm 0.9$ kΩ (**CARD-1C**). **CARD-1C** turned on and became readable by the SGS4 when it was exposed to the equilibrium vapor of $H_2O_2$ (35 wt% in water) and turned back off as it recovered under ambient atmosphere (Fig. 4 *B*, *2*). Although the exposures of **CARD-1C** to water, cyclohexanone, and $NH_3$ lead to small to moderate $\Delta R_s$ ($\Delta R_s = +1.5 \pm 0.6$ kΩ for water), these exposures did not invoke a change in its readability by SGS4 (Fig. 4 *B*, *1*, *3*, and *4*).

To detect cyclohexanone we fabricated a "turn-off" sensor **CARD-2** with an initial condition of being on by mechanical abrasion of **P2** at initial $R_s = 18.9 \pm 0.6$ kΩ on the surface of the tag. **CARD-2** turned off within 1 min of exposure to 335 ppm cyclohexanone (Fig. 4 *C*, *3*). The readability of **CARD-2** by SGS4 was reversible as it turned back on within 1 min of recovery under ambient air. The value of $R_s$ for **CARD-2**, however, did not recover to its initial value of $R_s$; rather, it settled at $R_s = 15.3 \pm 0.9$ kΩ after equilibrating for 10 min. We hypothesize that this mismatch in $R_s$ may be due to solvent-assisted rearrangement of the sensing material. Importantly, although exposure of **CARD-2** to $H_2O$, $H_2O_2$, and $NH_3$ produced small $\Delta R_s$ (Fig. 4 *C*, *1*, *2*, and *4*), they did not alter the readability of this sensor by the smartphone.

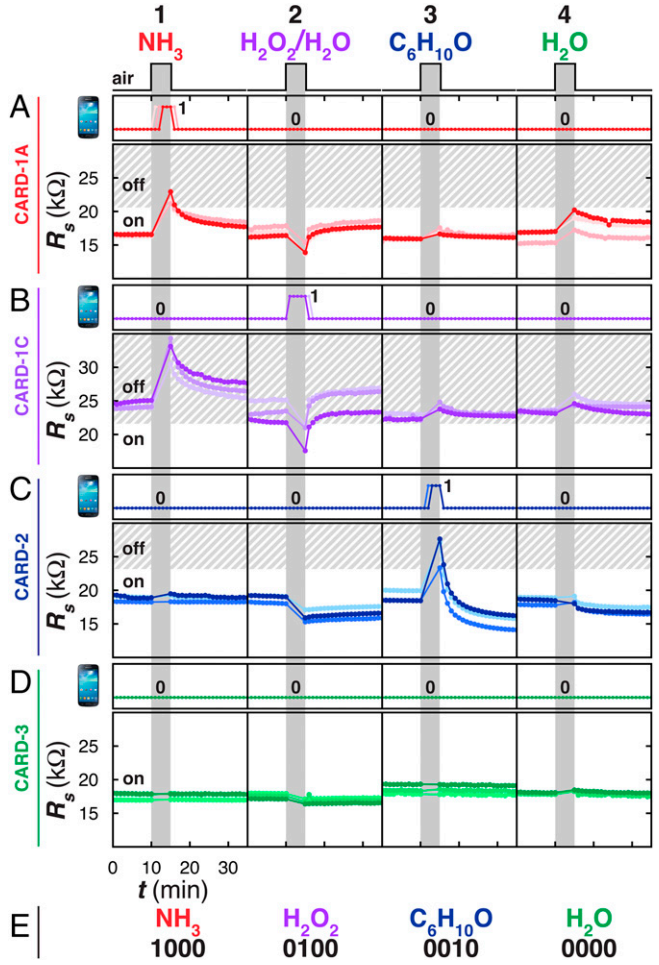


**Fig. 4.** Arrays of CARDs enable identification and discrimination of analytes. Response of programmed ($n = 3$) (*A*) **CARD-1A**, (*B*) **CARD-1C**, (*C*) **CARD-2**, and (*D*) **CARD-3** to single 5-min exposures of (1) $NH_3$ (35 ppm), (2) $H_2O_2$ (225 ppm), (3) cyclohexanone (335 ppm), and (4) $H_2O$ (30,000 ppm) as monitored with a SGS4 (*Top*) and multimeter (*Bottom*). Shaded boundary indicates estimated $R_t$ for each respective CARD based on the traces shown. Compiled binary SGS4 responses (*E*) of **CARD-1A**, **-1C**, **-2**, and **-3** codify the identity of the gases tested in this study.

As a negative control, we fabricated **CARD-3** by mechanical abrasion of **P3** to obtain $R_s = 18.0 \pm 0.6$ kΩ; this tag remained readable and did not change its readability in response to analytes used in this study (Fig. 4 *D*, *1–4*). This tag was an important component of an array-based sensing scheme because it validated the integrity of the reader-tag communication protocol and provided a static handle in a codification scheme.

The binary on/off readability of CARDs by the smartphone can be a powerful approach for converting analog physical inputs (presence or absence of a chemical vapor within a defined threshold) into a digitized output (1 and 0, respectively) that conveys meaningful information about the local chemical environment of the CARDs. The advantage of a binary readout is that it is the simplest possible output representation of input information, and hence allows modular multiplexing of different CARD combinations. Taken together, the data presented in Fig. 4 suggest that discrimination and identification of multiple analytes can be achieved with a smartphone by converting the output of binary CARDs (on/off) into multi-CARD logic (sequences of 0s and 1s) (Fig. 4*E*). This analytical approach has practical limitations in its implementation (see discussion in *Supporting Information*); however, it may be particularly useful in resource-constrained scenarios or high-throughput applications where information about the presence or absence of specific chemicals at specified thresholds is critically important. Such applications may include detection of an acceptable threshold (e.g., permissible exposure limit for a chemical) that provides valuable actionable information in dynamic, complex environments (e.g., chemical release within a public space). Even under circumstances wherein the chemical of interest can be readily detected by the human nose, a differentiating feature of a smartphone-based sensing strategy over human-olfactory detection or visual inspection of a colorimetric test is the ability to efficiently bring sensed information into the information technology infrastructure.

## Conclusion

We have developed an inexpensive, simple, rapid, and modular approach for converting commercially available NFC tags into chemically actuated devices that communicate with a smartphone via radio waves. This approach enables electronic wireless, non-line-of-sight detection and discrimination of gases and vapors at part-per-million and part-per-thousand concentrations. This technology provides binary (on/off) information about the presence or absence of a chemical analyte regarding designated concentration thresholds, (e.g., NIOSH STEL) within the local environment of the sensor tag and is capable of differentiating multiple concentrations of one analyte or multiple analytes using multi-CARD logic. The general sensing strategy involving wireless communication between NFC tags and smartphones is modular and can be generalized to incorporate many types of chemiresponsive materials to enable selective detection of diverse chemical changes. Nevertheless, addressing the significant challenges that remain to realize the full potential of this wireless sensing approach will require a cross-disciplinary effort of (*i*) chemical and materials science innovations to improve the sensitivity and selectivity of chemiresponsive materials to chemical analytes, (*ii*) improving device-to-device performance reproducibility by advancing the state-of-the-art of nanostructured carbon deposition techniques, and (*iii*) enabling continuum measurement CARD readout capabilities. The combination of chemical sensing with other capabilities within the smartphone (e.g., GPS) may enable additional utility in applications involving tracking and tracing. As a result of the portability and increasingly ubiquitous use of smartphones and mobile devices, we envision that this platform will enable applications in personalized and widely distributed chemical sensing where the acquisition of chemical or physical information was previously unattainable.

## Methods

**Conversion of a Commercial NFC Tag into a Programmable CARD.** The circuit of an NFC tag was disrupted at the location indicated in Fig. 1 using a circular hole puncher (hole diameter 2 mm; Bead Landing). A hole was punched through the tag, effectively removing a portion of the conducting aluminum film (along with the underlying polymeric substrate) connecting the integrated circuit to the capacitor. The circuit was recompleted via mechanical abrasion by drawing a line with an appropriate PENCIL to bridge the two disconnected ends of aluminum (17). An iterative process of mechanical abrasion of the PENCIL followed by measuring $R_s$ (Fig. S5) with a multimeter (Fluke 114 TRMS multimeter) was repeated until the desired initial $R_s$ value was achieved. When **P1**–**P3** are deposited on the surface of the NFC tag by mechanical abrasion they exhibit predictable drift characteristics, which allowed for the drawing of tags to predetermined specifications (Figs. S2 and S3). To prevent potential inhalation of particulates generated by the abrasion of PENCIL on NFC tags, this process was carried out in a fume hood. The resulting device was allowed to equilibrate until a stable reading ($\Delta R_s <$ 0.2 kΩ/10 min) was achieved (~30 min). All experiments were conducted within 5 h of making a CARD.

**Programming a CARD-Induced Smartphone Response.** As indicated in Movie S1, a response that is unique to a specific tag can be invoked upon successfully establishing communication between the tag and the phone (on/readable) by

ENGINEERING

preprogramming a tag-phone relationship before fabrication of a CARD. This study used the freely available application Trigger (Egomotion Corp.) to establish the phone-tag relationship. First, the unique identification number (UID) of a tag is registered with the smartphone by scanning it via NFC. Second, a task (or tasks) is assigned to that specific UID. For example, a task that can be achieved with the use of Trigger is to open another application, such as a note-taking application, that has a predefined message written on it. Other possible tasks that can be invoked include opening the email application with a prewritten message, opening a maps application that displays the current location of the smartphone, and so forth. By programming Trigger to invoke a unique task for each unique tag UID, once the tag has been converted to a CARD meaningful information about the CARD's chemical environment can be conveyed to the user. Although outside of the scope of this study, this strategy could be improved by creating a customized application that allows more sophisticated smartphone actions in a less cumbersome user-interface architecture.

**Method for Determining Reflection Coefficient and Readability of CARDs with a Smartphone.** The reflection coefficient spectra ($S_{11}$) were collected with a network analyzer (Agilent E5061B). A loop probe was affixed to the outside of a jar cap (250 mL; VWR) using electrical tape and a tag or CARD was placed on the inside of the same jar cap using double-sided tape (Fig. S4). Two jars were used for the experiment: one that was empty (i.e., filled with ambient air) and one that contained cyclohexanone (10 mL) and filter paper. The reflection coefficient spectra were measured and recorded once when the cap was on the empty jar, once after the cap was on the jar containing cyclohexanone for 5 s, and once after the cap was on the jar containing cyclohexanone for 1 min (Fig. 2*A*).

The readability of the tag or CARD was determined by removing the tag from the jar cap, placing it on a piece of open-cell foam (thickness 4.5 cm), and approaching the sensor tag with a Samsung Galaxy S4 running Android version 4.3 with the NFC Reader application (Adam Nybäck) open, held with its back parallel to the sensor tag. A sensor tag was considered on/readable if the UID could be retrieved within 5 s or less of holding the smartphone at a ~2.5-cm distance above the tag. Conversely, the tag was considered off/unreadable if the UID could not be retrieved under the same conditions. All measurements were performed with the phone oriented such that the parallel plate capacitor of the CARD was perpendicular to the long edge of the phone. The phone was held parallel to the surface on which the tag rested.

**Correlating Effects of Chemical Exposure on $R_s$ and Smartphone Readability of the CARD.** A CARD was attached to one side of a plastic Petri dish using double-sided tape. $R_s$ was determined by contacting the CARD at the indicated points using a multimeter (Fluke 114 TRMS multimeter). The readability of the CARD by SGS4 was determined as described above. Conversely, the CARD was considered off if the UID could not be retrieved under the same conditions.

First, we monitored $R_s$ and readability once a minute under ambient conditions to establish a stable baseline before chemical exposure for 10 min. Then, we exposed the tag to the chemical analyte by either placing the lid on a jar with saturated vapor ($H_2O_2/H_2O$ or $H_2O$) or in a zippered storage bag containing established atmosphere. During the chemical exposure the tag was not accessible to monitoring with a multimeter but it could still be interrogated with the smartphone at 1-min intervals. Once exposure was complete the tag was removed from the container and allowed to recover under ambient atmosphere. During this time, $R_s$ and readability were monitored at 1-min intervals.

**Binary Logic for Chemical Discrimination Using Arrays of CARDs.** Fig. 4*E* correlates the binary output of tag readability by the phone (on and off) with the identity of four chemical vapors used in this study. We use a binary (0 and 1) assignment in which the presence of a vapor is denoted as 1 and the absence of a vapor is denoted as 0. For example, in our demonstration we use four unique tags ($n = 4$), each programmed for a specific analyte or as a negative control. Because each tag has a unique identification number, the change in readability of each tag in response to a specified analyte is intrinsically linked to the identity and surmounted threshold of the vapor. We can arbitrarily arrange the $n$ sensor tags into a sequence to provide an $n$ digit code (###...) that can be used to identify unique gases and vapors. Using this coding scheme, four types of tags (**CARD-1A**, **-1C**, **-2**, and **-3**) and three types of vapors ($NH_3$, $H_2O_2$, and cyclohexanone), SGS4 can correctly identify the presence of 35 ppm $NH_3$ as 1000, the presence of vapor of 35% $H_2O_2$ dissolved in water as 0100, and the presence of 335 ppm cyclohexanone as 0010. As one of the most commonly encountered interferents, we emphasize that the presence of $H_2O$ vapor would not invoke a response from the sensor tags used in this study (0000). To enable a four-bit depth measurement, four individual CARDs need to be placed on a surface. The CARDs used in this study cover an area of 20.3 $cm^2$ each. Thus, four CARDs, which cannot be stacked on top of each other, would cover an area of 81.2 $cm^2$.

**ACKNOWLEDGMENTS.** J.B.R. thanks the Danish Council for Independent Research – Technology and Production. We thank NanoC for kindly providing single-walled carbon nanotubes for this project and Professor Steven Leeb for providing access to his network analyzer. This research was supported in part by the US Army Research Laboratory and the US Army Research Office through the Institute for Soldier Nanotechnologies under Contract W911NF-13-D-0001 (to J.M.A.), the Massachusetts Institute of Technology Deshpande Center for Technological Innovation (J.M.A.), and National Institutes of Health under Ruth L. Kirschstein National Research Service Award F32CA157197 from the National Cancer Institute (to K.A.M.).

1. Long F, Zhu A, Shi H (2013) Recent advances in optical biosensors for environmental monitoring and early warning. *Sensors (Basel)* 13(10):13928–13948.
2. Chen A, Chatterjee S (2013) Nanomaterials based electrochemical sensors for biomedical applications. *Chem Soc Rev* 42(12):5425–5438.
3. Kirsch J, Siltanen C, Zhou Q, Revzin A, Simonian A (2013) Biosensor technology: Recent advances in threat agent detection and medicine. *Chem Soc Rev* 42(22): 8733–8768.
4. Darwish A, Hassanien AE (2011) Wearable and implantable wireless sensor network solutions for healthcare monitoring. *Sensors (Basel)* 11(6):5561–5595.
5. Hakim M, et al. (2012) Volatile organic compounds of lung cancer and possible biochemical pathways. *Chem Rev* 112(11):5949–5966.
6. Potyrailo RA, et al. (2012) Wireless sensors and sensor networks for homeland security applications. *Trends Analyt Chem* 40:133–145.
7. Tothill IE (2001) Biosensors developments and potential applications in the agricultural diagnosis sector. *Comput Electron Agric* 30:205–218.
8. Potyrailo RA, Surman C, Nagraj N, Burns A (2011) Materials and transducers toward selective wireless gas sensing. *Chem Rev* 111(11):7315–7354.
9. Lee H, et al. (2011) Carbon-nanotube loaded antenna-based ammonia gas sensor. *Microw Theory Tech IEEE Trans* 59(10):2665–2673.
10. Potyrailo RA, et al. (2009) Development of radio-frequency identification sensors based on organic electronic sensing materials for selective detection of toxic vapors. *J Appl Phys* 106(12):124902.
11. Fiddes LK, Yan N (2013) RFID tags for wireless electrochemical detection of volatile chemicals. *Sens Actuators B Chem* 186:817–823.
12. Fiddes LK, Chang J, Yan N (2014) Electrochemical detection of biogenic amines during food spoilage using an integrated sensing RFID tag. *Sens Actuators B Chem* 202: 1298–1304.
13. Occhiuzzi C, Rida A, Marrocco G, Tentzeris MM (2011) Passive ammonia sensor: RFID tag integrating carbon nanotubes. *2011 IEEE Int Symp Antennas Propagation* (IEEE, New York), pp 1413–1416.
14. Nitkin PV, Rao KVS, Lazar S (2007) An overview of near field UHF RFID. *2007 IEEE Int Conf RFID* (IEEE, New York), pp 167–174.
15. Jing HC, Wang YE (2008) Capacity performance of an inductively coupled near field communication system. *2008 IEEE Antennas Propagation Soc Int Symp* (IEEE, New York), pp 1–4.
16. Mirica KA, Weis JG, Schnorr JM, Esser B, Swager TM (2012) Mechanical drawing of gas sensors on paper. *Angew Chem Int Ed Engl* 51(43):10740–10745.
17. Mirica KA, Azzarelli JM, Weis JG, Schnorr JM, Swager TM (2013) Rapid prototyping of carbon-based chemiresistive gas sensors on paper. *Proc Natl Acad Sci USA* 110(35): E3265–E3270.
18. Miyata Y, Maniwa Y, Kataura H (2006) Selective oxidation of semiconducting single-wall carbon nanotubes by hydrogen peroxide. *J Phys Chem B* 110(1):25–29.
19. Frazier KM, Swager TM (2013) Robust cyclohexanone selective chemiresistors based on single-walled carbon nanotubes. *Anal Chem* 85(15):7154–7158.
20. Cox JR, Müller P, Swager TM (2011) Interrupted energy transfer: Highly selective detection of cyclic ketones in the vapor phase. *J Am Chem Soc* 133(33):12910–12913.
21. Cole P, Ranasinghe D, Jamali B (2004) Coupling relations in RFID systems II: Practical performance measurements (Auto-ID Centre, Univ of Adelaide, Adelaide, SA, Australia).